

Optical Engineering

SPIDigitalLibrary.org/oe

Analytical model for the coupling constant of a directional coupler in terms of slab waveguides

Yann G. Boucher

Analytical model for the coupling constant of a directional coupler in terms of slab waveguides

Yann G. Boucher

CNRS, UMR 6082 FOTON, CS 80518, Lannion cedex F-22305, France

Abstract. We present an analytical model for a generic two-wave directional coupler, in the conceptual frame of coupled single-mode planar (slab) waveguides. The modal relation of dispersion is expressed exactly under a matrix form. In the simplest symmetric configuration, the lift of degeneracy between the propagation constants of the even (slow) and odd (fast) supermodes is the exact image of the coupling constant. © 2014 Society of Photo-Optical Instrumentation Engineers (SPIE) [DOI: [10.1117/1.OE.53.7.071810](https://doi.org/10.1117/1.OE.53.7.071810)]

Keywords: integrated optics; glass photonics; slab waveguides; coupled-mode theory.

Paper 131665SS received Nov. 1, 2013; revised manuscript received Dec. 14, 2013; accepted for publication Dec. 18, 2013; published online Jan. 13, 2014.

1 Introduction

Directional coupler is a key element for many photonic systems, from integrated beam-splitters to Mach-Zehnder interferometers,¹⁻³ including the input/output ports of microresonators. The total fraction of power that can be transmitted, along with the relative phase of the outgoing waves, is the crucial parameter for evaluating the system performance. In a similar fashion, the quality factor and the spectral properties of a microresonator rely heavily on the coupler.⁴⁻⁸ Whatever the context, the underlying physical mechanism is often the same: otherwise isolated waveguides are brought in close vicinity along a finite interaction length, over which guided modes can exchange energy due to a mutual overlap of their evanescent parts.

Evaluating the scattering parameters of a given coupler is a mandatory step before any successful designing. Since these depend critically on optogeometrical parameters (such as dimensions, indices, etc.), extensive numerical calculation is often required. Nevertheless, it is always very instructive to use a simple analytical model that gives the general tendency with respect to any change of wavelength, material, or geometry.

In this respect, coupled-mode theory (CMT) is an attractive as well as a powerful tool for describing the exchange between two waveguides over a given interaction length.^{1,2,9-11} In the canonical (“textbook”) case of two single-mode parallel waveguides, the problem is completely determined by two dimensionless parameters only: the integrated coupling constant (with a strength proportional to the mutual overlap) and the overall detuning between the propagation constants of the two waveguides.

These quantities can either be evaluated approximately in the frame of a perturbative approach, or calculated numerically, or even determined experimentally. By contrast, what we attempt in the present work is to establish an analogical model for a directional coupler between two single-mode symmetrical waveguides, in the frame of a matrix formalism that enables one to determine “exactly” (i.e., in a “non-perturbative” way) the precise value of the coupling constant, by extracting it from the modal relation of dispersion of the whole structure.

The paper is organized as follows. In Sec. 2, we recall the main formal results relative to CMT, and the expression of the coupling constants as seen through the prism of a perturbation approach. In Sec. 3, we expose the matrix formalism that gives the relation of dispersion, and we show how it can be used to extract the coupling constant of a two-waveguide symmetrical system without any approximation. We comment on the transverse profile of the even and odd supermodes and investigate the evolution of the coupling constants as a function of the gap between the two waveguides. Since our original motivation was to dispose of a rapid model for describing the coupling between a tapered fiber and a SiO₂ spherical microresonator,⁸ all numerical applications are relative to glass/air structures. The case of “weighted coupling,” where the system exhibits a (slow) longitudinal variation of the gap along the propagation axis, is briefly commented upon in Sec. 4. Conclusions and perspectives are given in Sec. 5.

2 CMT Formalism and Perturbative Approach

Notations may vary according to the authors, but the principles remain the same and are very well documented.^{1,2,9-11} Consider two parallel, lossless, single-mode waveguides exchanging their fields over interaction length L along the z -axis, as schematically depicted in Fig. 1. Let β_p denotes the propagation constant of waveguide $n^o p$, and $\beta = (\beta_1 + \beta_2)/2$; time dependence is taken as $\exp(+i\omega t)$. Wavelength and wave-vector in vacuum are λ_0 and $k_0 = (\omega/c)$.

2.1 Coupled-Mode Theory

When the waveguides are isolated,

$$i \frac{\partial}{\partial z} \begin{pmatrix} F_1 \\ F_2 \end{pmatrix} = \begin{pmatrix} \beta_1 & 0 \\ 0 & \beta_2 \end{pmatrix} \begin{pmatrix} F_1 \\ F_2 \end{pmatrix}, \quad (1)$$

so that each mode propagates with its own propagation constant. In the presence of mutual coupling, the problem can usually be reduced to:

Address all correspondence to: Yann G. Boucher, E-mail: boucher@enib.fr

0091-3286/2014/\$25.00 © 2014 SPIE

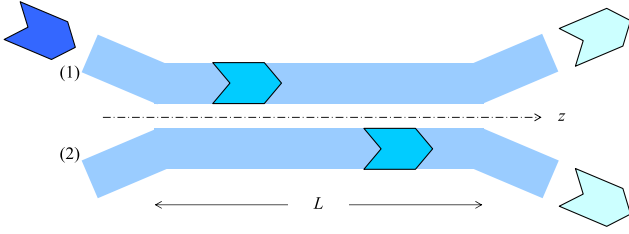


Fig. 1 Coupling between waveguides Nos. 1 and 2 over an interaction length L .

$$i \frac{\partial}{\partial z} \begin{pmatrix} F_1 \\ F_2 \end{pmatrix} = \begin{pmatrix} \beta_1 & \chi \\ \chi & \beta_2 \end{pmatrix} \begin{pmatrix} F_1 \\ F_2 \end{pmatrix}, \quad (2)$$

where the nondiagonal “perturbation” term is responsible for coupling. The “textbook” problem¹⁻³ is completely determined by two parameters: detuning $\Delta = (\beta_1 - \beta_2)/2$ and coupling constant χ , which can be considered as real and positive without loss of generality. The slowly varying field envelopes A_p , such as $F_p = A_p \exp(-i\beta z)$, are easily shown to obey:

$$i \frac{\partial}{\partial z} \begin{pmatrix} A_1 \\ A_2 \end{pmatrix} = \begin{pmatrix} \Delta & \chi \\ \chi & -\Delta \end{pmatrix} \begin{pmatrix} A_1 \\ A_2 \end{pmatrix}, \quad (3)$$

so that A_1 and A_2 are both solutions to the following second-order ordinary differential equation (ODE), where $\Gamma = [\chi^2 + \Delta^2]^{1/2}$:

$$\frac{\partial^2 A_p}{\partial z^2} + \Gamma^2 A_p = 0. \quad (4)$$

Taking into account the initial conditions $F_1(0) = F_{10}$, $F_2(0) = F_{20}$, it is straightforward to establish the relationship:

$$\begin{pmatrix} F_{1L} \\ F_{2L} \end{pmatrix} = e^{-i\beta L} \begin{pmatrix} \cos(\Gamma L) - i \frac{\Delta}{\Gamma} \sin(\Gamma L) & -i \frac{\chi}{\Gamma} \sin(\Gamma L) \\ -i \frac{\chi}{\Gamma} \sin(\Gamma L) & \cos(\Gamma L) + i \frac{\Delta}{\Gamma} \sin(\Gamma L) \end{pmatrix} \begin{pmatrix} F_{10} \\ F_{20} \end{pmatrix}. \quad (5)$$

For perfect phase-matching ($\Delta = 0$, so that $\Gamma = \chi$), its expression is even simpler

$$\begin{pmatrix} F_{1L} \\ F_{2L} \end{pmatrix} = e^{-i\beta L} \begin{pmatrix} \cos(\chi L) & -i \sin(\chi L) \\ -i \sin(\chi L) & \cos(\chi L) \end{pmatrix} \begin{pmatrix} F_{10} \\ F_{20} \end{pmatrix}. \quad (6)$$

It is interesting to note the formal similarity with a “Jones-type” matrix, describing the effect of an anisotropic plate in polarization optics. The exchange of energy over distance is illustrated in Fig. 2 for different values of the reduced detuning (Δ/χ), in the special case where the only input field is injected into waveguide No. 1 at $z = 0$ ($F_{10} = 1$, $F_{20} = 0$).

Only for perfect phase matching, can one expect to couple 100% of energy from one guide to the other. Otherwise, the maximum amount of coupled power is given by

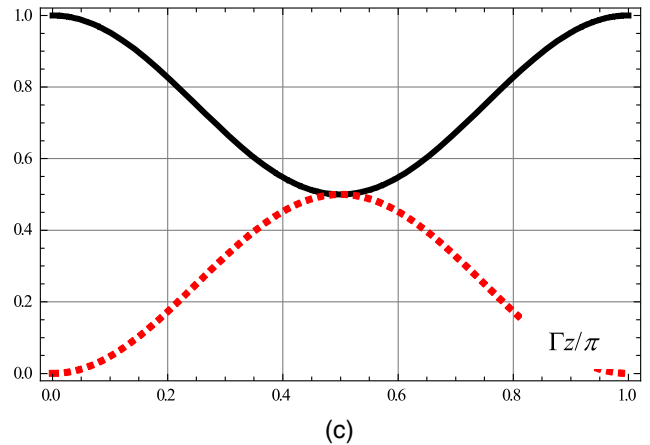
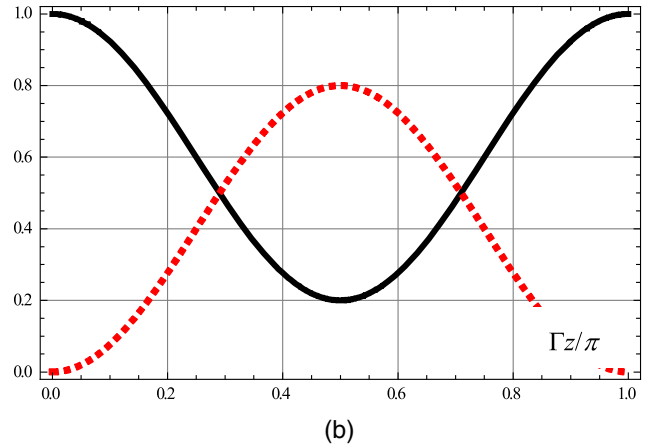
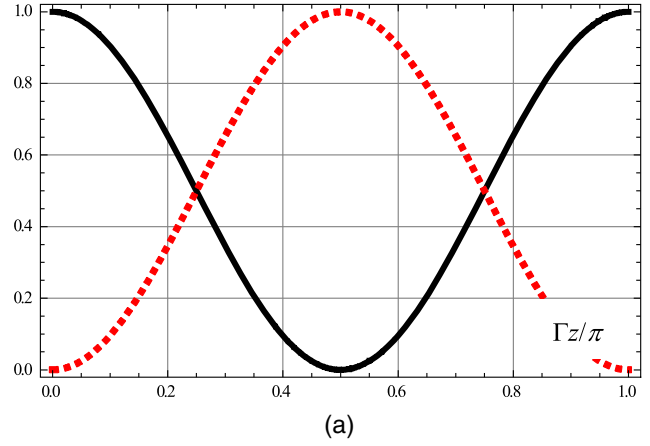


Fig. 2 Periodic exchange of power between waveguides as a function of distance z : $|F_1(z)|^2$ (black line) and $|F_2(z)|^2$ (red dotted line) for $F_{10} = 1$ and $F_{20} = 0$. (a) Perfect phase matching ($\Delta/\chi = 0$); (b) Phase mismatch $\Delta/\chi = 0.5$; (c) phase mismatch $\Delta/\chi = 1$.

$$\eta = \frac{\chi^2}{\chi^2 + \Delta^2}. \quad (7)$$

It should be noted that total conversion is rarely required. If only a few percent need to be exchanged, phase matching is definitely “not” an issue. This should be kept in mind when dealing with high- Q microresonators, where too strong a coupling could lead to a dramatic decrease of the Q -factor: in such a case, phase matching is not a relevant requirement.

On the other hand, the phase-matched case exhibits another interesting property: the eigenmodes of the superstructure are either symmetric (even) or antisymmetric (odd). They are, respectively, characterized by propagation constants β_e (the slow mode) and β_o (the fast mode) such as $\beta_e - \beta_o = 2\chi$. These play a role quite similar to the slow and fast waves in an anisotropic plate. Note also that the lift of degeneracy from one double value of β into a couple (β_e, β_o) is the formal equivalent, in the spatial frequency domain, of the Rabi splitting of *Quantum Mechanics* in the spectral domain.¹² This universal phenomenon, affecting any kind of coupled resonators, has the same algebraic basis: it stems from the diagonalization of a nondiagonal matrix.

2.2 Perturbative Approach

Following Yariv and Yeh,¹ consider two parallel single-mode cylindrical waveguides (Fig. 3).

For negligible coupling, let (β_a, β_b) denote their respective propagation constants. In the perturbative approach, the total field propagating along the z -axis can be written as:

$$\mathbf{E} = A(z)\mathbf{E}_a(x, y)e^{-i\beta_a z} + B(z)\mathbf{E}_b(x, y)e^{-i\beta_b z}, \quad (8)$$

where $\mathbf{E}_a(x, y)$ and $\mathbf{E}_b(x, y)$ denote the profile of the modes supported by the isolated waveguides. The coupling is responsible for the “variation of constants” $A(z)$ and $B(z)$, representing slowly varying amplitudes. Inserting Eq. (8) into the propagation equations, neglecting the second derivatives and projecting onto the relevant modes, we get eventually

$$\begin{cases} i\frac{\partial A}{\partial z} = \chi_{aa}A + \chi_{ab}B e^{i(\beta_a - \beta_b)z} \\ i\frac{\partial B}{\partial z} = \chi_{bb}B + \chi_{ba}A e^{-i(\beta_a - \beta_b)z} \end{cases}, \quad (9)$$

where the four parameters χ_{uv} can be expressed as overlap integrals:

$$\begin{cases} \chi_{ab} = \frac{\omega\epsilon_0}{4} \int \mathbf{E}_a^* \cdot \Delta n_a^2(x, y) \mathbf{E}_b dx dy \\ \chi_{ba} = \frac{\omega\epsilon_0}{4} \int \mathbf{E}_b^* \cdot \Delta n_b^2(x, y) \mathbf{E}_a dx dy \end{cases}, \quad (10)$$

$$\begin{cases} \chi_{aa} = \frac{\omega\epsilon_0}{4} \int \mathbf{E}_a^* \cdot \Delta n_b^2(x, y) \mathbf{E}_a dx dy \\ \chi_{bb} = \frac{\omega\epsilon_0}{4} \int \mathbf{E}_b^* \cdot \Delta n_a^2(x, y) \mathbf{E}_b dx dy \end{cases}. \quad (11)$$

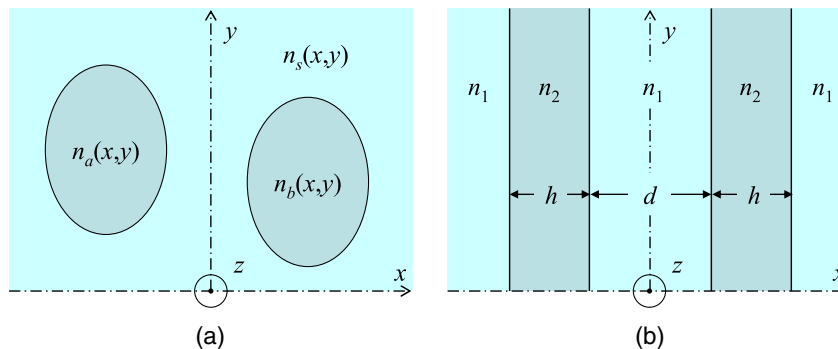


Fig. 3 Schematic depiction of two parallel single-mode cylindrical waveguides. (a) General case and (b) symmetrical slab waveguides.

The first two terms stand for mutual coupling, and the last two terms stand for “diagonal” coupling.

In the symmetrical configuration (two identical waveguides), $\chi_{ab} = \chi_{ba} = \chi$, and $\chi_{aa} = \chi_{bb}$. The initial detuning $\Delta = (\beta_a - \beta_b)/2 = 0$ remains therefore unchanged: phase matching is automatically observed. One can also note that Eq. (9) does not exhibit the same form as Eq. (1), since evolution operator retains a z -dependence. A change of variables is necessary to recover an “invariant” evolution operator. Let $\beta = (\beta_a + \beta_b)/2$ denotes the initial average propagation constant, and $\beta' = \beta + (\chi_{aa} + \chi_{bb})/2$ denotes its new (corrected) value; if (A_1, A_2) are chosen such as $A(z)\exp(-i\beta_a z) = A_1(z)\exp(-i\beta' z)$ and $B(z)\exp(-i\beta_b z) = A_2(z)\exp(-i\beta' z)$, these must follow Eq. (3) with $\Delta = 0$.

In the special case of slab structures, the existence of known solutions for the mode supported by each isolated waveguide leads to explicit expressions for the coupling constants. For instance, in the symmetric case, Yariv and Yeh¹ show that χ presents an exponential decrease with the distance d between the waveguides.

But slab waveguides prove very convenient for yet another reason: the coupling constant can be recovered exactly, without any restriction pertaining to the perturbative approximation. This is the subject of Sec. 3.

3 Symmetrical Slab Waveguides: Non-Perturbative Approach

3.1 Slab Waveguides and Matrix Formalism

Consider the isolated slab waveguide as illustrated in Fig. 4.

From an electromagnetic point of view, it is easy to separate the two eigenstates of polarization, using the electric field $\mathbf{E} = E(x)\mathbf{e}_y$ in the TE case, the magnetic field $\mathbf{H} = H(x)\mathbf{e}_y$ in the TM case. We look for propagative solutions in the guiding region (the core), for evanescent solutions in the surrounding cladding. Dropping a common factor $\exp(+i\omega t - i\beta z)$, we write the transverse part of the “wave function” in zone p as the superposition of two parts, ψ_p^+ and ψ_p^- , with $\psi_p^+ = A_p \exp(-i\kappa z)$ and $\psi_p^- = B_p \exp(+i\kappa z)$ if propagation, $\psi_p^+ = A_p \exp(-\gamma z)$ and $\psi_p^- = B_p \exp(+\gamma z)$ if evanescence, with $\beta^2 - \gamma^2 = k_1^2 = n_1^2 k_0^2$, $\beta^2 + \kappa^2 = k_2^2 = n_2^2 k_0^2 > k_1^2$.

The continuity of Maxwell’s equations and the boundary conditions (no exponential increase in a semi-infinite cladding) enable one to express the relationship between the fields in a matrix way:

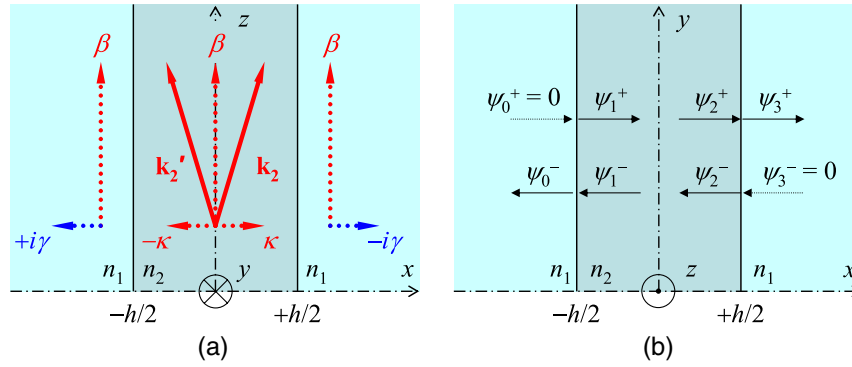


Fig. 4 Isolated symmetric slab waveguide of index n_2 and thickness h , surrounded by a medium of index n_1 . (a) seen from above, with the transverse and longitudinal parts of the wave-vectors; (b) cross-section, with the wave-functions at each interface.

$$\begin{pmatrix} 0 \\ \psi_0^- \end{pmatrix} = \begin{pmatrix} m_{11} & m_{12} \\ m_{21} & m_{22} \end{pmatrix} \begin{pmatrix} \psi_3^+ \\ 0 \end{pmatrix}, \quad (12)$$

where

$$[m] = \begin{pmatrix} \cos \kappa h - \frac{1}{2} \left(\rho - \frac{1}{\rho} \right) \sin \kappa h & -\frac{1}{2} \left(\rho + \frac{1}{\rho} \right) \sin \kappa h \\ \frac{1}{2} \left(\rho + \frac{1}{\rho} \right) \sin \kappa h & \cos \kappa h + \frac{1}{2} \left(\rho - \frac{1}{\rho} \right) \sin \kappa h \end{pmatrix}, \quad (13)$$

with

$$\rho_{\text{TE}} = \frac{\mu_1 \kappa}{\mu_2 \gamma} = \frac{\mu_1 \kappa h}{\mu_2 \gamma h}, \quad \rho_{\text{TM}} = \frac{\varepsilon_1 \kappa}{\varepsilon_2 \gamma} = \frac{\varepsilon_1 \kappa h}{\varepsilon_2 \gamma h}. \quad (14)$$

The modal resonance condition reads:

$$m_{11} = 0. \quad (15)$$

From this equation, one can extract the discrete (quantized) values of κh corresponding to each mode. If the reduced parameter $V = k_0 h [n_2^2 - n_1^2]^{1/2}$ is inferior to π , the guide is intrinsically single mode (actually, it supports one mode for each state of polarization). Once κ is known, so is β , since $\beta^2 + \kappa^2 = k_2^2$. Propagation constant is customarily written as $\beta = n_{\text{eff}}(\omega/c)$, where n_{eff} is the effective index of the given mode. We draw in Fig. 5 the TE mode profile at $\lambda_0 = 1.5 \mu\text{m}$ for a single-mode slab waveguide defined by $n_1 = 1$, $n_2 = 1.5$, $h = 0.67 \mu\text{m}$. All subsequent numerical applications are relative

to the same set of parameters. The evanescent part is clearly visible outside the core region, explaining the overlap mechanism with any added external layer.

3.2 Coupled Symmetrical Slab Waveguides

The same principle holds for the coupled structure represented in Fig. 3(b), except for the detail of the matrix calculation. In the symmetrical case, the relevant matrix is $[M]$ such as

$$[M] = [m] \begin{pmatrix} \exp(+\gamma d) & 0 \\ 0 & \exp(-\gamma d) \end{pmatrix} [m], \quad (16)$$

and the modal condition reads

$$M_{11} = 0, \quad (17)$$

which is equivalent to

$$m_{11} = \pm m_{21} e^{-\gamma d}. \quad (18)$$

The solutions are depicted graphically in Fig. 6. For great enough distances ($\gamma d \gg 1$), the waveguides remain uncoupled: the solutions are that of an isolated waveguide. For smaller gaps, the degeneracy is clearly lifted (although not necessarily in a symmetric way). The former value of κh is replaced by a couple $(\kappa_e h, \kappa_o h)$ corresponding to even and odd solutions, with $\kappa_e < \kappa_o$.

It is instructive to follow the profile of the super-modes, for decreasing values of the gap d (Fig. 7). For the sake of

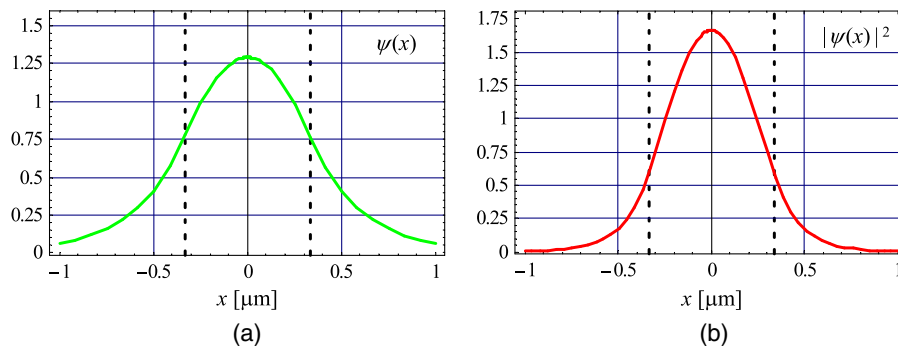


Fig. 5 Mode profile of the fundamental (and only) mode, for $\lambda_0 = 1.5 \mu\text{m}$, $n_1 = 1$, $n_2 = 1.5$, $h = 0.67 \mu\text{m}$. (a) amplitude $\psi(x) = \psi^+(x) + \psi^-(x)$; (b) intensity, normalized such as $\int |\psi(x)|^2 dx = 1$.

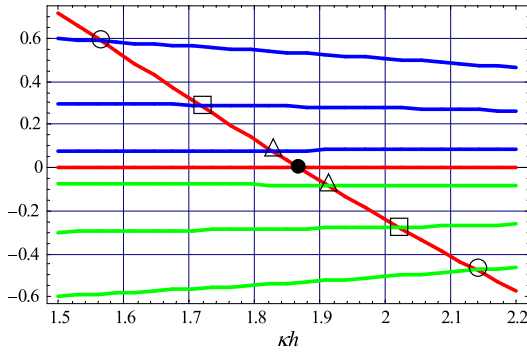


Fig. 6 Graphical depiction of solutions for various values of d : m_{11} , $m_{21}e^{-\gamma d}$, $-m_{21}e^{-\gamma d}$ as a function of κh ; isolated guide ($m_{11} = 0$, dark circles), $(d/h) = 1$ (triangles), $(d/h) = 1/2$ [squares] et $(d/h) = 1/4$ [open circles]. The closer the guides, the greater the lift of degeneracy.

clarity, we draw the amplitude $\psi(x)$ as well as the intensity $|\psi(x)|^2$, in order to clearly distinguish the even from the odd behavior.

We would like to point out that in the limiting case of a vanishingly small gap ($d = 0$), where treating the neighboring waveguide as a mere “perturbation” would make no sense, the modal condition retains all its meaning: the structure has become a single waveguide of thickness $2h$, supporting two modes. The even and odd “super-modes” have actually merged into the lower and higher modes of the bimodal waveguide.

Since (κ_e, κ_o) are unequivocally determined, it is straightforward to extract the corresponding propagation constants (β_e, β_o) along the z -axis, with $\beta_e > \beta_o$. As a consequence, we get

$$\chi = \frac{\beta_e - \beta_o}{2}, \quad (19)$$

$$\beta' = \frac{\beta_e + \beta_o}{2}. \quad (20)$$

The coupling constant is drawn in Fig. 8(a) as a function of d . By the way of comparison, we also represent the perturbative value as calculated following Yariv and Yeh;¹ with our notations:

$$\chi = \frac{2\kappa^2\gamma \exp(-\gamma d)}{\beta(h + \frac{2}{\gamma})(\kappa^2 + \gamma^2)}. \quad (21)$$

We also obtain the new value of the average propagation constant, as corrected by the (otherwise unknown) “diagonal” term χ_{aa} (see Sec. 2.2). As can be seen from Fig. 8(b), it differs significantly from the perturbative model, where a monotonically decreasing behavior in $\exp(-2\gamma d)$ is expected.

We would like to emphasize the following points:

- Normalized coupling constant χh appears bounded by an upper limit, that is obtained for $d = 0$.
- In that configuration, the system is formally reduced to a unique waveguide of thickness $2h$ ($V \approx 2\pi$), therefore supporting two modes instead of one:

- Conversely, any two-mode slab waveguides can be thought of as a set of two highly coupled single-mode waveguides.
- More generally, for a given state of polarization, any multimode slab waveguide (of thickness H) supporting N modes is formally equivalent to a set of N coupled single-mode waveguides (of individual thickness H/N).
- The evolution of χ with d still plainly follows an exponential law $\chi_0 e^{-\gamma d}$, even for a vanishingly small gap between waveguides, in a clearly “non-perturbative” regime, that is, very far from “the assumption that the waveguides are not too close, so that the overlap integral of the mode functions is small!”.
- On the other hand, the “diagonal correction” transforming β into β' exhibits a non-intuitive behavior that cannot be recovered by a mere overlap integral (which would monotonically decrease as $e^{-2\gamma d}$); however, this term remains small (about 1‰ in our case) and becomes negligible as soon as $d \geq h$.

One can also note that the upper value of χ is directly connected to the difference between the two quantized values of κ in a bimodal waveguide since $\beta_e^2 + \kappa_e^2 = \beta_o^2 + \kappa_o^2 = k_2^2$, we get:

$$\chi = \frac{\beta_e - \beta_o}{2} = \frac{\kappa_o^2 - \kappa_e^2}{4\beta'}. \quad (22)$$

Bearing in mind that the order of magnitude of $(\kappa_o h - \kappa_e h)$ is π , we obtain a rough but very convenient estimation of the coupling range accessible with a given geometry.

The explicit exponential evolution of χ with d opens the way to the study of structures that are no longer invariant with respect to the z -axis as long as their longitudinal variation remains reasonably small.

4 Weighted Coupling: Some Exact Solutions

4.1 Longitudinally Varying Evolution Operator

In some instances, we have to deal with a longitudinal gradient of coupling, for instance, if the gap d varies with abscissa z . In the case of a reasonably slow gradient (the slope of the variation remaining much smaller than the other relevant parameters), we retrieve a typical case of “weighted coupling” (see, e.g., Tamir et al.²): in first approximation, the integrated coupling strength χL is simply replaced by an effective value $(\chi L)_{\text{eff}} = \int \chi(z) dz$. It is possible to go a step further by deriving the propagation equation, which is shown to admit exact solutions in some typical cases.

From a formal point of view, let us assume two identical waveguides symmetrically coupled by a z -dependent coupling “constant” $\chi(z)$. Slowly varying amplitudes (A_1, A_2) are subject to:

$$i \frac{\partial}{\partial z} \begin{pmatrix} A_1 \\ A_2 \end{pmatrix} \equiv \begin{pmatrix} 0 & \chi(z) \\ \chi(z) & 0 \end{pmatrix} \begin{pmatrix} A_1 \\ A_2 \end{pmatrix}. \quad (23)$$

After some elementary algebra, the ODE simultaneously verified by both A_p reads:

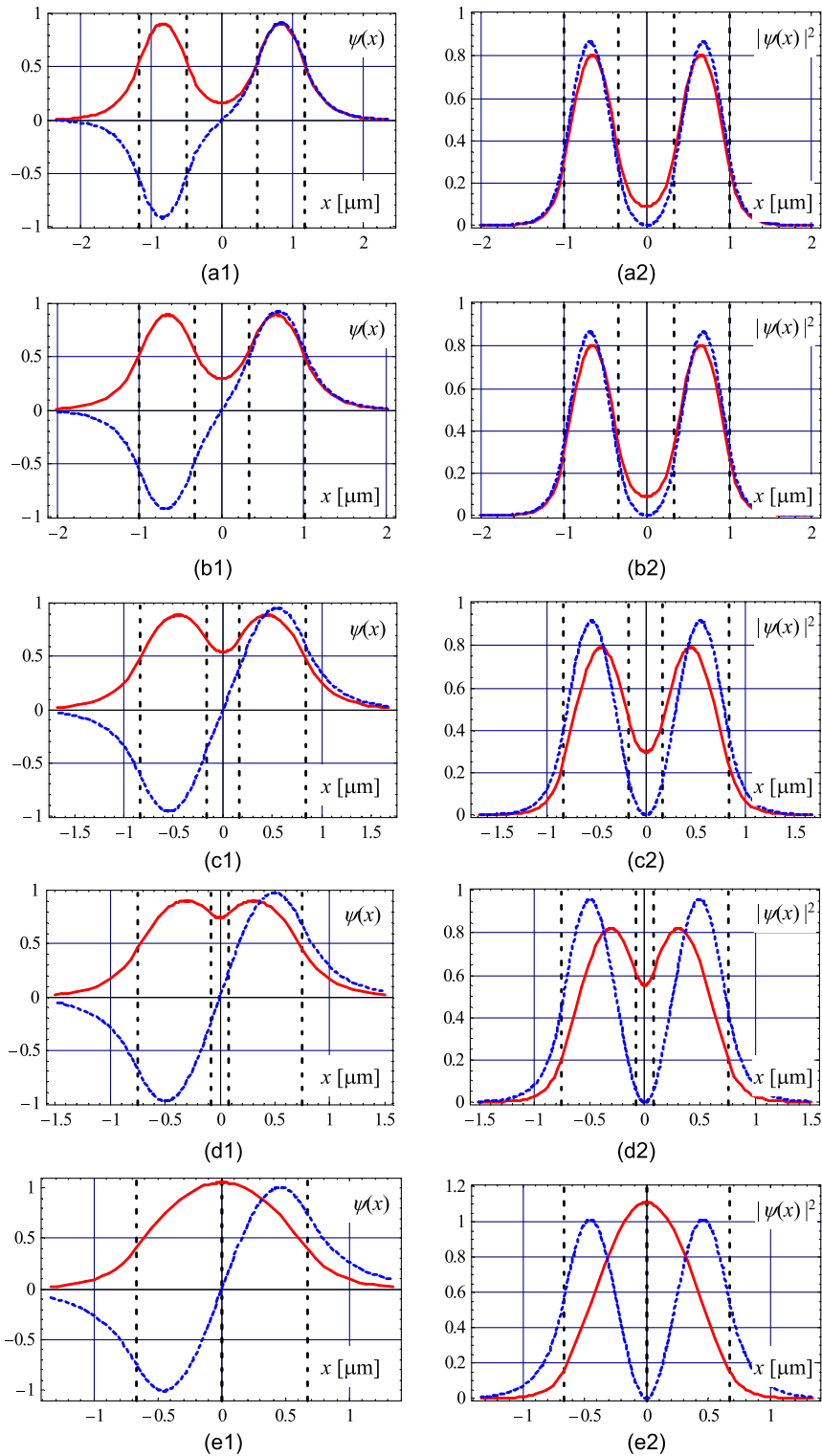


Fig. 7 Profile of the even (in red) and odd (in blue) supermodes, for (a) $d = 3h/2$, (b) h , (c) $h/2$, (d) $h/4$, and (e) $d = 0$. Left column (a1 to e1): amplitude $\psi(x)$; right column (a2 to e2): normalized intensity $|\psi(x)|^2$.

$$\frac{\partial^2 F}{\partial z^2} - \frac{1}{\chi} \left(\frac{\partial \chi}{\partial z} \right) \frac{\partial F}{\partial z} + \chi^2 F = 0. \quad (24)$$

For simple variations (linear or quadratic) of $\chi(z)$, this ODE admits exact solutions.

4.2 Linear Variation of the Gap

We assume a linear variation of distance d , written as

$$d(z) = d_i + d_0 \left(\frac{z}{z_0} \right), \quad (25)$$

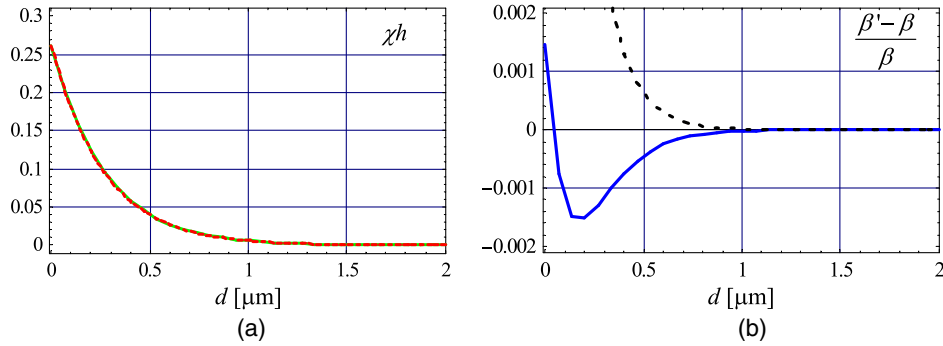


Fig. 8 (a) Evolution of normalized coupling constant χh with gap d , as compared with an exponential law $(\chi_0 h) \exp(-\gamma d)$; (b) Relative correction to the average propagation constant $(\beta' - \beta)/\beta$ as a function of d , as compared to the perturbative limit, monotonically decreasing as $\exp(-2\gamma d)$.

over the whole interaction zone ($z \in [0, L]$), as depicted in Fig. 9.

As a result, coupling constant evolves as $\chi(z) = \chi_i e^{-z/a}$, where χ_i is the initial value and $a = z_0/(\gamma d_0)$ is the characteristic length. Equation (24) becomes

$$\frac{\partial^2 F}{\partial z^2} + \frac{1}{a} \frac{\partial F}{\partial z} + \chi_i^2 e^{-2z/a} F = 0. \quad (26)$$

Its general solution reads

$$F(z) = k_a \cos[\chi_i a e^{-z/a}] + k_b \sin[\chi_i a e^{-z/a}], \quad (27)$$

where k_a and k_b are integration constants that depend on boundary conditions.

The general solution can be written under a matrix form as

$$\begin{pmatrix} A_1(z) \\ A_2(z) \end{pmatrix} = \begin{pmatrix} \cos[\Phi(z)] & -i \sin[\Phi(z)] \\ -i \sin[\Phi(z)] & \cos[\Phi(z)] \end{pmatrix} \begin{pmatrix} A_{10} \\ A_{20} \end{pmatrix}, \quad (28)$$

$$\begin{pmatrix} F_1(z) \\ F_2(z) \end{pmatrix} = e^{-i\beta z} \begin{pmatrix} \cos[\Phi(z)] & -i \sin[\Phi(z)] \\ -i \sin[\Phi(z)] & \cos[\Phi(z)] \end{pmatrix} \begin{pmatrix} F_{10} \\ F_{20} \end{pmatrix}, \quad (29)$$

$$\Phi(z) = \chi_i a (1 - e^{-z/a}). \quad (30)$$

Comparing with Eq. (6), one can see that this matrix has exactly the same form as in the z -invariant case, except for the replacement rule $\chi z \rightarrow \Phi(z)$. The maximum value of the coupling strength is $(\chi L)_{\text{eff}} = \chi_i a$. The variation of $\Phi(z)$ is depicted in Fig. 10.

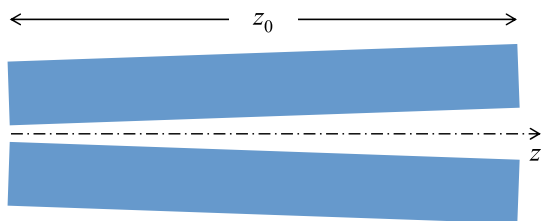


Fig. 9 Symmetrical coupler with linear variation of gap d with respect to z .

4.3 Quadratic Variation of the Gap

We assume now a quadratic variation of distance d , written as

$$d(z) = d_i + d_0 \left(\frac{z^2}{2z_0^2} \right), \quad (31)$$

over the whole interaction zone ($z \in [0, L]$), as depicted in Fig. 11.

As a result, coupling constant evolves in a Gaussian way as $\chi(z) = \chi_i \exp[-(z/a)^2]$, where χ_i is the initial value and a is the characteristic length, such as $a^2 = 2z_0^2/(\gamma d_0)$. Equation (24) becomes

$$\frac{\partial^2 F}{\partial z^2} + \frac{2z}{a^2} \frac{\partial F}{\partial z} + \chi_i^2 e^{-2(z/a)^2} F = 0. \quad (32)$$

Its general solution reads

$$F(z) = k_a \cos \left[\frac{\chi_i a \sqrt{\pi}}{2} \text{Erf} \left(\frac{z}{a} \right) \right] + k_b \sin \left[\frac{\chi_i a \sqrt{\pi}}{2} \text{Erf} \left(\frac{z}{a} \right) \right], \quad (33)$$

where k_a and k_b are integration constants that depend on boundary conditions.

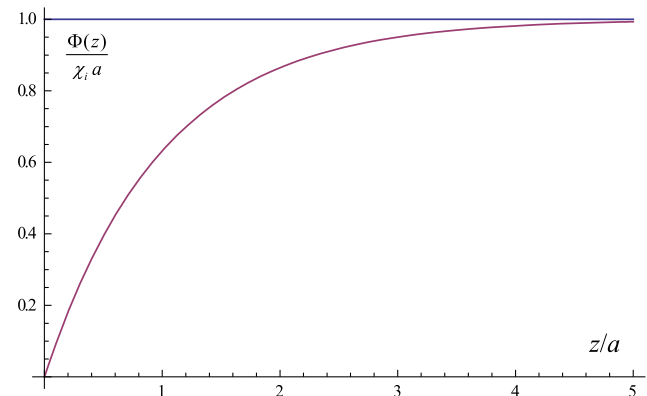


Fig. 10 Evolution of $\Phi(z)$ in the linear case.

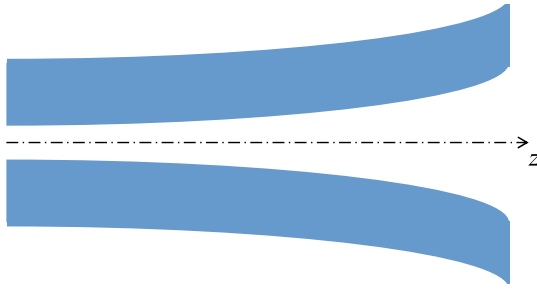


Fig. 11 Symmetrical coupler with quadratic variation of gap d with respect to z .

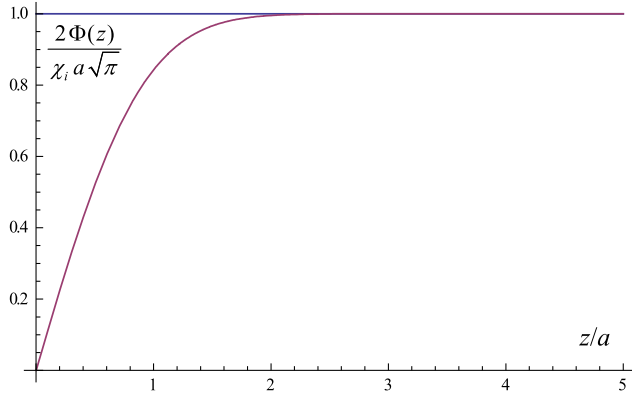


Fig. 12 Evolution of $\Phi(z)$ in the quadratic case.

Once again, the general solution can be written under a matrix form as

$$\begin{pmatrix} F_1(z) \\ F_2(z) \end{pmatrix} = e^{-i\beta z} \begin{pmatrix} \cos[\Phi(z)] & -i \sin[\Phi(z)] \\ -i \sin[\Phi(z)] & \cos[\Phi(z)] \end{pmatrix} \begin{pmatrix} F_{10} \\ F_{20} \end{pmatrix}, \quad (34)$$

$$\Phi(z) = \frac{\chi_i a \sqrt{\pi}}{2} \text{Erf} \left(\frac{z}{a} \right). \quad (35)$$

The variation of $\Phi(z)$ is depicted in Fig. 12.

The conclusion is the same as before, with a maximum value of coupling

$$(\chi L)_{\text{eff}} = \frac{\chi_i a \sqrt{\pi}}{2}. \quad (36)$$

In both cases, it can be interpreted in terms of an “effective coupling length” after which the waveguides become too far from each other to interact. Note that the quadratic case can be used as a first approximation for modeling the coupling between a single-mode straight waveguide and a single-mode ring-like resonator (ring, disk, or sphere), provided the curvature is not too pronounced.

5 Conclusions

In the typical case of symmetrically coupled single-mode slab waveguides, we have derived the coupling constant in a rigorous way, without any need to resort to the usual

perturbative approximation. As a matter of fact, coupling constant χ is an exact image of the lift of degeneracy between the slow (even) and fast (odd) super-modes of the whole structure. We have also found that χ is bounded by a finite upper limit.

From a fundamental point of view, for a given eigen-state of polarization (TE or TM), any multimode slab waveguide (of thickness H) supporting N modes can be thought of as a system of N mutually coupled single-mode waveguides (of individual thickness H/N). It should be noted that, for purely formal reasons of matrix symmetry, this holds also true for an electronic wave-function inside a quantum well (QW), where bound states obey a modal equation similar to Eq. (15)¹³: any multiple-state QW can be seen as resulting from the coupling of smaller single-state QW.

Although all the simulations have been presented for a given wavelength, we would like to emphasize that modal dispersion $\chi(\omega)$ can be extracted in the same way. Since we work in the spectral domain, taking material dispersion into account is also straightforward. The influence of geometrical parameters (indices, thickness, gap) is immediately clear, since all expressions are derived analytically, with the only exception of the modal condition, which requires the resolution of a transcendental equation.

We have not only derived a very simple model bearing great physical insight, we have also shown that codirectional CMT remains soundly valid even in the non-perturbative regime, much longer than usually believed. This is not as surprising as it may seem, since CMT expresses the fact that the eigen-functions of a linear system can be expressed as a superposition of the eigen-functions of its parts like a molecular orbital constructed as a linear combination of atomic orbitals. Basically, it stems from the linearity of electromagnetism and should hold as long as the exchange remains linear. One should also mention that in quite another context, that of contra-directional coupling, two-mode CMTs are already known to hold in distributed Bragg reflectors with an arbitrary high index contrast,¹⁴ opening a fascinating new field of investigation.¹⁵

One can ask oneself how the slab picture would be modified if some symmetry were broken. Actually, in the case of non-identical slab waveguides (different indices or thicknesses), deriving the modal condition remains straightforward, but extracting simultaneously the coupling constant χ as well as the detuning Δ requires some precaution: another condition may be called for. This problem is currently under investigation.

Acknowledgments

This work has been partially supported by research projects ANR-BLANC-2010-0312-1 (ORA) and CNES R&T R-S10/LN-0001-004 (SHYRO), as well as by Région Bretagne through its research network “RTR Siscom.” The author would like to thank Prof. Patrice Féron (FOTON Laboratory, CNRS, Lannion) and Dr. Arnaud Fernandez (LAAS Laboratory, CNRS, Toulouse) for stimulating discussions.

References

1. A. Yariv and P. Yeh, *Optical Waves in Crystals*, Wiley, New York (1984).
2. Th. Tamir, Ed., *Guided-Wave Optoelectronics*, Springer-Verlag, Berlin (1988).

3. C.-L. Chen, *Foundations for Guided-Wave Optics*, Wiley, New York (2006).
4. V. B. Braginsky, M. L. Gorodetsky, and V. S. Ilchenko, "Quality-factor and nonlinear properties of optical whispering-gallery modes," *Phys. Lett. A* **137**(7–8), 393–397 (1989).
5. K. Vahala, Ed., *Optical Microcavities*, World Scientific Publishing, Singapore (2004).
6. J. Heebner, R. Grover, and T. Ibrahim, *Optical Microresonators: Theory, Fabrication, and Applications*, Springer-Verlag, London (2010).
7. D. G. Rabus, *Integrated Ring Resonators: The Compendium*, Springer-Verlag, Berlin (2010).
8. G. Righini et al., "Whispering gallery mode microresonators: fundamentals and applications," *Riv. Nuovo Cimento* **34**(7), 435–488 (2011).
9. A. Yariv, "Coupled mode theory for guided-wave optics," *IEEE J. Quantum Electron.*, **9**(9), 919–933 (1973).
10. A. Hardy and W. Streifer, "Coupled mode theory of parallel waveguides," *J. Lightw. Technol.* **3**(5), 1135–1146 (1985).
11. H. A. Haus et al., "Coupled-mode theory of optical waveguides," *J. Lightw. Technol.* **5**(1), 16–23 (1987).
12. C. Cohen-Tannoudji, B. Diu, and F. Laloë, *Quantum Mechanics*, Wiley, New York (1977).
13. E. Rosencher and B. Vinter, *Optoelectronics*, Cambridge University Press, Cambridge (2002).
14. N. Matuschek, F. X. Kärtner, and U. Keller, "Exact coupled-mode theories for multilayer interference coatings with arbitrary strong index modulations," *IEEE J. Quantum Electron.* **33**(3), 295–302 (1997).
15. Y. G. Boucher, "Fundamentals of couplonics," *Proc. SPIE* **6182**, 61821E (2006).

Yann G. Boucher is an assistant professor based in Lannion, FOTON Laboratory, for his research, and in Brest for his teaching. He received his Ingénieur degree from École Supérieure d'Optique, Orsay, in 1988, and his PhD degree from Paris-Sud University, Orsay, in 1993. His current research interests include analytical modeling of photonic integrated devices. He is a member of SPIE, IEEE Photonics Society, the European Optical Society, and the Optical Society of America.